

# Multivariate analysis of dynamical processes

## Point processes and time series

K. Henschel<sup>1,2,a</sup>, B. Hellwig<sup>3</sup>, F. Amtage<sup>3</sup>, J. Vesper<sup>3</sup>, M. Jachan<sup>1</sup>, C.H. Lücking<sup>3</sup>,  
J. Timmer<sup>1,2</sup>, and B. Schelter<sup>1</sup>

<sup>1</sup> FDM, Freiburg Center for Data Analysis and Modeling, University of Freiburg, Eckerstr. 1,  
79104 Freiburg, Germany

<sup>2</sup> Bernstein Center for Computational Neuroscience, Hansastr. 9A,  
79104 Freiburg, Germany

<sup>3</sup> Neurology Department, University Hospital of Freiburg, Breisacherstr. 64,  
79110 Freiburg, Germany

**Abstract.** The analysis of multi-dimensional biomedical systems requires analysis techniques, which are able to deal with multivariate data consisting of both time series as well as point processes. Univariate and bivariate analysis techniques in the frequency domain for time series and point processes are established and investigated, although the number of investigations is strongly biased towards time series. Actual multivariate techniques for time series or hybrids of time series and point processes are scarcely addressed. Here, we present spectral analysis techniques which are able to analyse point processes as well as time series. Thereby, univariate, bivariate as well as multivariate techniques are discussed. Applications to simulated as well as real-world data reveal the abilities of the proposed techniques.

## 1 Introduction

Recordings of multivariate datasets are omnipresent in many fields of research. For a better understanding of the underlying system, say a biomedical network, univariate, bivariate, and recently multivariate analysis techniques have been proposed [1–3]. It is not clear in the first place how to extend these methods to the case where the observed processes are point processes. In contrast to a time series, point processes are sequences of events. The information is encoded solely by the times of the occurrences of these events. Point processes are of particular interest in neuroscience due to the fact that interactions and information processing of neurons is realised by point processes, i.e. the instants in time when action potentials are generated. Multivariate time series analysis techniques, applicable to point processes, would allow for inference of the network structure of neuronal networks. Whenever the interplay between neuronal activity and time series has to be addressed, a further adaptation of the techniques to cope with hybrids of time series and point processes is mandatory. A hybrid of time series and point processes is for instance recorded in tremor research. During stereotactic neurosurgery neuronal activity as well as muscular activity is recorded, whereby the latter represents a time series. The analysis techniques summarised and introduced in this work are applied to simulated data and the tremor example mentioned above.

---

<sup>a</sup> e-mail: [henschel@fdm.uni-freiburg.de](mailto:henschel@fdm.uni-freiburg.de)

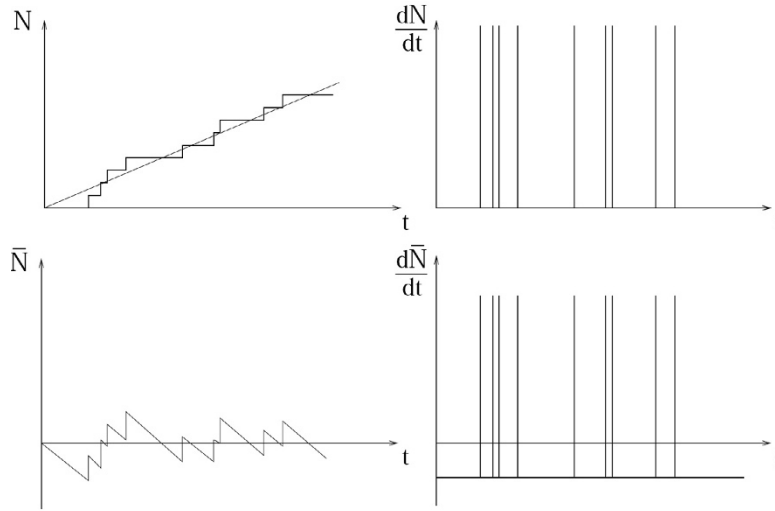


**Fig. 1.** Subtraction of the mean of a point process. Upper row: Counting process  $N(t)$  (trend indicated in grey) and its derivative  $\frac{dN}{dt}$ . Lower row: Counting process  $\bar{N}(t)$  (trend subtracted) and its derivative.

## 2 Fourier transform for time series and point processes

For a time series  $x(t)$  of length  $N$  and sampling rate  $1/\Delta t$  the Fourier transform is given by

$$\mathcal{FT}\{x(t)\}(\omega) = \frac{1}{\sqrt{\pi N}} \sum_{j=1}^N e^{-i\omega j \Delta t} x(j \Delta t), \quad (1)$$

with natural frequency values  $\omega_k = \frac{2\pi k}{N \Delta t} = \frac{2\pi}{T} k$ ,  $k = -\frac{N}{2} \dots, 0, \dots, \frac{N}{2}$  where  $N \Delta t = T$  is the length of the time series.

Since point processes are characterised by a sequence of events, the notion of time series is no longer valid. Several approaches have been discussed to calculate the Fourier transform of a point process. A common idea is to convert the point process into a time series to make it accessible for the well-investigated methods in the framework of time series analysis. This conversion can be implemented by binning or by a convolution with an appropriate kernel function [4, 5].

The application of the binning method requires a careful choice of the binning width to avoid aliasing effects. The aliasing effect is long known for time series. Assume that for instance a biomedical system under investigation contains frequencies of a certain band width. Assume further that this process is sampled at frequency  $f_s$ . At least two scenarios are now conceivable. Firstly, the frequency band of the biomedical system is lower than twice the sampling frequency. In this case all frequencies can be analysed by spectral analysis. Secondly, the sampling frequency is too low, i.e. it is lower than twice the upper bound of the frequency band. In this case, spectral analysis will yield false positive informations about the frequencies contained in the signal. Components of the signal with a frequency  $f_0$  higher than the Nyquist frequency  $f_{Ny}$  will contribute to the Fourier transform at  $f_{Ny} - f_0$  leading to strongly biased estimators of, for instance, the spectrum (see below). The Nyquist frequency is given by

$$f_{Ny} = \frac{f_s}{2}, \quad (2)$$

with  $f_s$  denoting the sampling frequency. For time series it is necessary to low pass filter the data before sampling with a cut off frequency smaller than the Nyquist frequency.

For point processes there is no natural analogue to the Nyquist frequency since point processes are not sampled like time series. When transforming the point processes into time

series the binning introduces however an artificial Nyquist frequency. To ensure an unbiased estimator of, for instance, the spectrum, as a thumb rule this Nyquist frequency can be chosen to be the 3- to 7-fold of the characteristic frequency  $f_{\max}$  of the process. This characteristic frequency can be determined if there is prior knowledge about the characteristic time intervals  $T_{\text{char}}$  of the process and therefore of  $f_{\max} = 1/T_{\text{char}}$ . Alternatively, it is possible to choose a small binning width to ensure that there are mainly zeros and only very few ones in the time series, which in turn ensures a sufficiently high sampling rate.

If there is no prior knowledge about the process, data driven concepts to derive an equation for the Nyquist frequency implicitly are conceivable. However, to avoid the problems described above emerging from the conversion of the point process to a time series, Fourier transformation and therefore spectral estimation should be performed directly on the point process.

To this aim, an intuitive notion of point processes is given by the number of events  $N_t = \sum_s \Theta(t - T_s)$  that occurred until time  $t$ . The Heaviside function  $\Theta(x)$  takes the value one for  $x > 0$ , zero otherwise. Thereby, the times  $T_s$  denote the occurrence of events. The expectation value of  $N_t$  for a stationary point process is given by

$$\mathcal{E}\{N_t\} = \lambda t. \quad (3)$$

The quantity  $\lambda$  is called the intensity of the point process, which can be interpreted as the firing rate of the point process. For the increment process of the point process we obtain a series of Dirac- $\delta(\cdot)$  functions

$$dN_t = \sum_s \delta(t - T_s) dt. \quad (4)$$

The Fourier transform of the point process of length  $T$  is then straight forward

$$\mathcal{FT}\{dN_t\}(\omega) = \frac{1}{\sqrt{\pi T}} \int e^{-i\omega t} dN_t, \quad (5)$$

$$= \frac{1}{\sqrt{\pi T}} \sum_s e^{-i\omega T_s}. \quad (6)$$

However, this definition has the disadvantage that for  $\omega = 0$  every single addend in the sum equals one, which would lead to a singularity for  $\omega = 0$ . This in turn leads to overestimated spectral values for low frequencies.

To overcome this limitation, it is important to subtract the mean of the point process. The centred point process  $\bar{N}_t = N_t - \lambda t$  with expectation value  $\mathcal{E}\{d\bar{N}_t/dt\} = 0$  is considered. In the case of a stationary point process the intensity can be estimated via  $\hat{\lambda} = N_T/T$ .

The Fourier transform [6]

$$\mathcal{FT}\{d\bar{N}_t\}(\omega) = \frac{1}{\sqrt{\pi T}} \int e^{-i\omega t} d\bar{N}_t, \quad (7)$$

$$= \frac{1}{\sqrt{\pi T}} \int e^{-i\omega t} [dN_t - \lambda dt], \quad (8)$$

$$= \frac{1}{\sqrt{\pi T}} \left[ \sum_s e^{-i\omega T_s} - 2\pi\lambda\delta(\omega) \right], \quad (9)$$

reveals periodicities in the occurrence of events that lead to an increase in the correlation at that specific frequency with respect to the correlation expected by chance alone.

### 3 Spectral estimation

Here we address the differences in the spectral estimation between time series and point processes.

### 3.1 Spectral estimation for time series

The spectrum of a process can be defined as the expectation value of its periodogram

$$S(\omega_k) = \mathcal{E} \{ \text{Per}_x(\omega_k) \}. \quad (10)$$

The periodogram is given by [9]

$$\text{Per}_x(\omega_k) = |\mathcal{FT}\{x(t)\}(\omega_k)|^2, \quad (11)$$

with  $\omega_k = \frac{2\pi k}{N\Delta t}$ ,  $k = 1, \dots, \frac{N}{2}$  and  $\Delta t$  denoting the sampling width. However, for finite realisations of this process, i.e. the time series, an estimator for the spectrum has to be introduced. Given a zero mean time series  $x(t)$  of length  $N$  of a stationary process, fulfilling certain mixing conditions [7], the spectrum can be estimated by smoothing the periodogram [4,8]. Using a smoothing window  $w_j$  of width  $2s + 1$  which has to fulfil  $\sum_j w_j = 1$ , for example a triangular window, the estimate of the spectrum is given by

$$\hat{S}_x(\omega_k) = \sum_{j=-s}^s w_j \text{Per}_x(\omega_{k+j}) = \sum_{j=-s}^s w_j |\mathcal{FT}\{x(t)\}(\omega_{k+j})|^2. \quad (12)$$

To avoid leakage effects the time series should be tapered with an appropriate window function.

The confidence interval of the spectral estimate for a significance level  $\alpha$  is given by

$$\left( \frac{\nu \hat{S}_x(\omega_k)}{\chi_\nu^2(1 - \frac{\alpha}{2})}, \frac{\nu \hat{S}_x(\omega_k)}{\chi_\nu^2(\frac{\alpha}{2})} \right). \quad (13)$$

Thereby  $\nu$  denotes the equivalent number of degrees of freedom. For the calculation of  $\nu$  the smoothing and taper window have to be taken into account [9].

### 3.2 Spectral estimation for point processes

Analogously to the spectrum of processes generating time series, the spectrum of a point process can be directly estimated via smoothing the periodogram. The periodogram of the tapered point process is given by

$$\text{Per}_{\tilde{N}_t}(\omega) = \left| \mathcal{FT}\{\widetilde{d\tilde{N}_t}\}(\omega) \right|^2, \quad (14)$$

with

$$\mathcal{FT}\{\widetilde{d\tilde{N}_t}\}(\omega) = \frac{1}{\sqrt{\pi T}} \int h(t) e^{-i\omega t} [dN(t) - \hat{\lambda} dt], \quad (15)$$

$$= \frac{1}{\sqrt{\pi T}} \left[ \sum_s h(T_s) e^{-i\omega T_s} - \hat{\lambda} H(\omega) \right], \quad (16)$$

whereby  $H(\omega)$  denotes the Fourier transform of the taper window  $h(t)$ . For  $h(t)$  the normalisation

$$\int_0^T h^2(t) dt = T, \quad (17)$$

is necessary to guarantee a correct normalisation of the spectrum.

The spectral estimation for a point process is finally given by

$$\hat{S}_{\tilde{N}_t}(\omega_k) = \sum_{j=-s}^s w_j \text{Per}_{\tilde{N}_t}(\omega_{k+j}), \quad (18)$$

with  $\omega_k = 2\pi k/T$  for a point process of length  $T$ .

## 4 Bivariate analysis

### 4.1 Cross spectrum and coherence for point processes

Cross-spectral analysis for time series is a common methodology to analyse the linear relationship between two time series in the frequency domain [4]. Having in mind the previously stated findings concerning the univariate analysis of point processes, it is possible to establish estimators for the cross-periodogram, cross-spectrum, and coherence for point processes.

The cross-periodogram of two point processes  $N_t$  and  $M_t$  can be defined as

$$\text{CPer}_{\bar{N}_t \bar{M}_t}(\omega_k) = \mathcal{FT}\{\widetilde{d\bar{N}_t}\} \mathcal{FT}^*\{\widetilde{d\bar{M}_t}\}. \quad (19)$$

Please note that for time series the very same equation holds with substituting the point processes  $N_t$  and  $M_t$  by time series  $x(t)$  and  $y(t)$ . To obtain a consistent estimator for the cross-spectrum, the cross-periodogram has to be smoothed as described above

$$\text{CS}_{\bar{N}_t \bar{M}_t}(\omega_k) = \sum_{j=-s}^s w_j \text{CPer}_{\bar{N}_t \bar{M}_t}(\omega_{k+j}). \quad (20)$$

Rescaling the smoothed cross-spectrum with respect to the auto-spectra yields the coherence

$$\widehat{\text{Coh}}_{\bar{N}_t \bar{M}_t}(\omega_k) = \frac{\left| \sum_{j=-s}^s w_j \text{CPer}_{\bar{N}_t \bar{M}_t}(\omega_{k+j}) \right|}{\sqrt{\hat{S}_{\bar{N}_t}(\omega_k) \hat{S}_{\bar{M}_t}(\omega_k)}}, \quad (21)$$

between the point processes  $M_t$  and  $N_t$ . The real and imaginary part of the cross-periodogram have to be smoothed.

### 4.2 Point processes and time series

The coherence between a time series and a point process can be estimated by conversion of the point process into a time series and application of the methods for time series or again by using the actual Fourier transform of the point process itself. For the latter the cross-periodogram

$$\text{CPer}_{x(t)\bar{N}_t}(\omega) = \mathcal{FT}\{x(t)\}(\omega) \mathcal{FT}^*\{\widetilde{d\bar{N}_t}\}(\omega), \quad (22)$$

is calculated.

## 5 Multivariate techniques

In this section we present multivariate techniques that allow for distinguishing direct and indirect as well as the direction of interactions in multivariate networks consisting of both point processes and time series.

### 5.1 Partial coherence

For a network of interacting neurons the described bivariate analysis is not able to discriminate direct from indirect interactions. If, for example, two mutually independent processes are influenced by a third one, bivariate analysis will also detect a connection between the former and therefore yield misleading results [1].

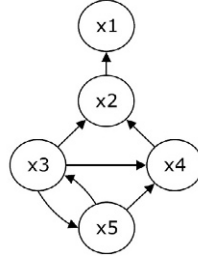


**Fig. 2.** 5-dim network of connected neurons. The direct directed interactions are indicated by arrows.

To distinguish direct and indirect connections partial coherence has been suggested [2,3]. The main idea is to subtract the linear information of all remaining possibly multi-dimensional processes  $y(t)$  from the considered processes  $x_a(t)$  and  $x_b(t)$ . In the frequency domain, partial coherence is based on partial cross and auto-spectra. The partial cross-spectrum can be evaluated by [2]

$$CS_{x_a x_b | y}(\omega) = CS_{x_a x_b}(\omega) - CS_{x_a y}(\omega) S_{yy}^{-1}(\omega) CS_{y x_b}(\omega). \quad (23)$$

Rescaling the partial cross-spectrum by the partial auto-spectra  $S_{x_a x_a | y}$ , leads to the partial coherence

$$\text{Coh}_{x_a x_b | y}(\omega) = \frac{|CS_{x_a x_b | y}(\omega)|}{\sqrt{S_{x_a x_a | y}(\omega) S_{x_b x_b | y}(\omega)}}. \quad (24)$$

The estimation of partial coherence can be implemented via inversion and rescaling of the spectral matrix

$$\mathbf{S}(\omega) = \begin{pmatrix} S_{x_1 x_1}(\omega) & CS_{x_1 x_2}(\omega) & CS_{x_1 x_3}(\omega) & \cdots & CS_{x_1 x_k}(\omega) \\ CS_{x_2 x_1}(\omega) & S_{x_2 x_2}(\omega) & \cdots & \cdots & \vdots \\ \vdots & \cdots & \ddots & \cdots & \vdots \\ \vdots & \cdots & \cdots & \ddots & \vdots \\ CS_{x_k x_1}(\omega) & \cdots & \cdots & \cdots & S_{x_k x_k}(\omega) \end{pmatrix}, \quad (25)$$

whose entries contain the auto-spectra on the diagonal and the cross-spectra on the off-diagonal elements [2].

To demonstrate the performance of partial coherence, we simulated a five-dimensional network of neurons. Each simulated neuron was influenced by its own activity through a refractory period and the activity of other neurons. To implement the refractory period of the neurons, which is a short period of time after an event occurred in which no second event can occur, their spontaneous firing rate was set to zero directly after each event. During the refractory period with a duration of 10 ms, the firing rate slowly increases until it again reaches the spontaneous firing rate. The influence of one neuron onto the others was implemented by increasing the firing rate of the influenced neurons once the driver fired. The simulated network is depicted in Fig. 2. Figure 3 shows the estimated coherence and partial coherence values from a realisation of this multivariate network with a spontaneous firing rate of 0.1 per ms and a duration of 5s. All coherence values in Fig. 3 (above the diagonal) are significantly different from zero. Therefore, a bivariate analysis does not reveal the correct interaction structure but detects a fully connected network; thus yields false positive results. In contrast, the network structure is correctly detected by partial coherence analysis (Fig. 3 – below the diagonal). Several partial coherence values are compatible with zero indicating an indirect interaction between the processes as for instance between processes 1 and 4. The partial coherence introduced above is directly applicable to time series as well. Since only the Fourier transformed processes enter the analysis, networks consisting of time series, point processes, and hybrids thereof can be readily analysed. Although this method yields information whether a link is direct or not, with respect

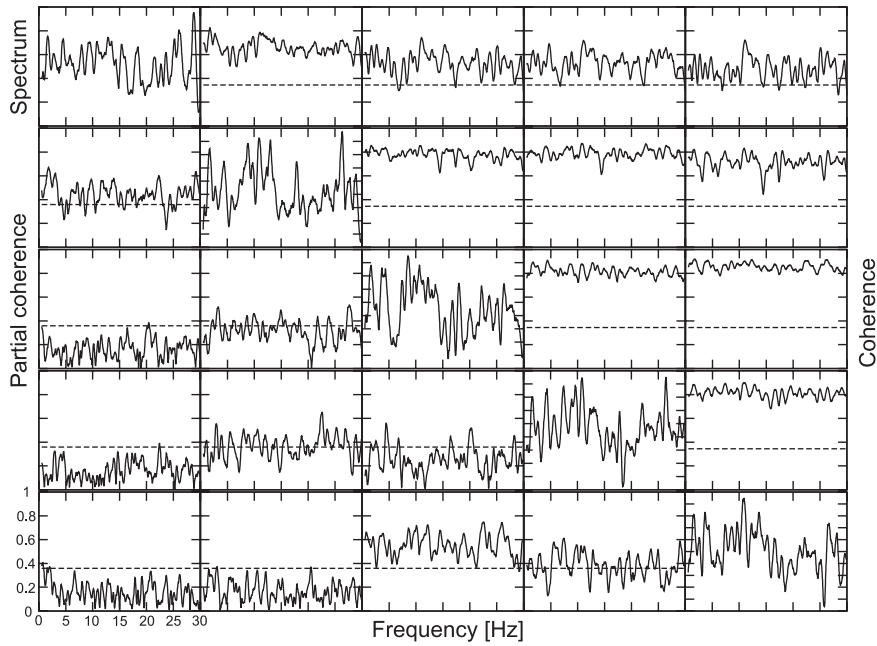


**Fig. 3.** Estimated coherence (above diagonal) and partial coherence (below diagonal) spectra. The spectra of the processes are shown on the diagonal. The interaction structure depicted in Fig. 2 is correctly reproduced. The horizontal lines represent the 99% level of significance.

to the other observed processes, the question of the direction of information flow still remains open.

## 5.2 Renormalized partial directed coherence

Besides the information whether or not a link is direct, the direction of the information flow is often of particular interest. An approach to infer direct directed interactions in multivariate datasets is given by partial directed coherence (PDC) which was suggested in [10,11]. The concept is based on linear Granger causality, modelled by underlying vector autoregressive process of order  $p$  (VAR[ $p$ ]).

The VAR[ $p$ ] representation of an  $n$ -dimensional system is

$$\begin{pmatrix} x_1(t) \\ \vdots \\ x_n(t) \end{pmatrix} = \sum_{u=1}^p \mathbf{a}(u) \begin{pmatrix} x_1(t-u) \\ \vdots \\ x_n(t-u) \end{pmatrix} + \begin{pmatrix} \epsilon_1(t) \\ \vdots \\ \epsilon_n(t) \end{pmatrix}. \quad (26)$$

Using the Fourier transform of the coefficient matrices  $\mathbf{a}(u)$

$$\mathbf{A}(\omega) = I - \sum_{u=1}^p \mathbf{a}(u) e^{-i\omega u} \quad (27)$$

the partial directed coherence can be evaluated as

$$|\pi_{i \leftarrow j}(\omega)| = \frac{|\mathbf{A}_{ij}(\omega)|}{\sqrt{\sum_k |\mathbf{A}_{kj}(\omega)|^2}}. \quad (28)$$

Coefficients  $\pi_{i \leftarrow j}(\omega)$  significantly larger than zero indicate a direct linear influence of process  $j$  onto process  $i$  at a given frequency  $\omega$ . Due to some weaknesses in the normalisation of the

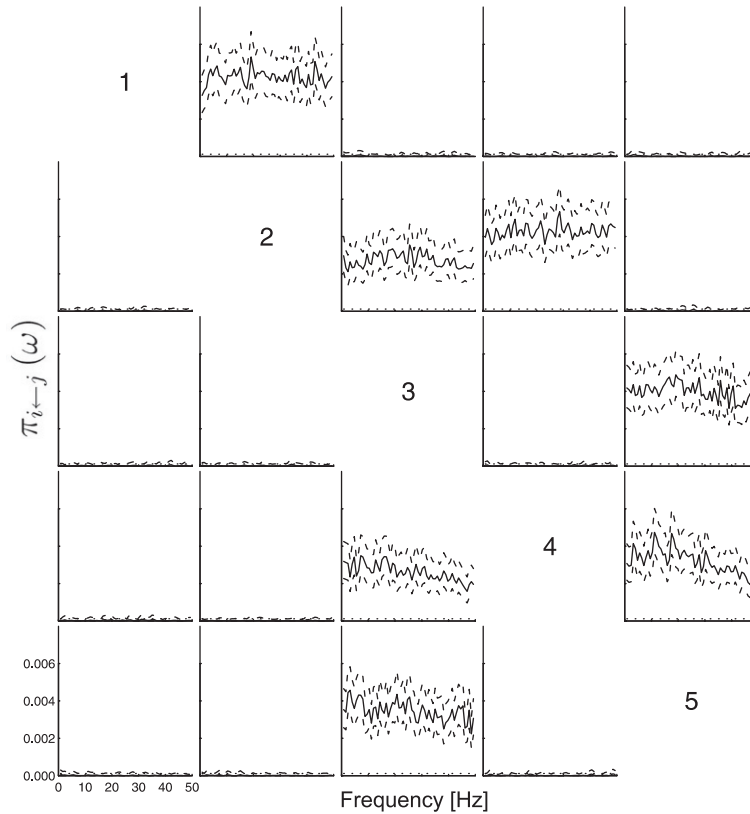


**Fig. 4.** Estimates of rPDC for the simulated network. Neuronal processes were converted to 0-1 time series to make them accessible for auto regressive modelling. The partial directed coherence value  $\pi_{i \leftarrow j}$ , belonging to the direct directed influence from process  $j$  onto process  $i$ , is depicted in the  $i$ th row and  $j$ th column of the matrix of rPDC spectra. The horizontal dotted line represents the 99% significance level, while the dashed lines are the 99% confidence intervals. The topology of the simulated network shown in Fig. 2 is correctly reproduced including the directions of information transfer.

PDC, the interpretability of the PDC is hampered. An alternative normalisation procedure is suggested in [12] to obtain the so-called renormalised partial directed coherence (rPDC). The rPDC was applied to the network of neurons described above. The estimated rPDC values are depicted in Fig. 4. They correctly reveal the simulated network structure including the directions of information transfer.

## 6 Application to a tremor network

To demonstrate the performance of the rPDC on real-world data we used data recorded from patients suffering from Parkinsonian tremor. Tremor is one of the cardinal symptoms of Parkinson's disease and manifests itself predominantly in the trembling of the upper limbs. The trembling frequency lies between 3 Hz and 8 Hz.

The data used for the analysis was gathered during stereotactic neurosurgery. Neuronal activity was recorded using five microelectrodes that were placed in the subthalamic nucleus (STN), a brain region assumed to be involved in tremor generation. Neuronal activity was extracted from the microelectrode recordings using a spike sorting algorithm [13]. The activity of the trembling muscles was recorded simultaneously using surface electromyography (EMG) electrodes. The EMG recordings were high-pass filtered to remove movement artefacts, rectified, and corrected for the mean.

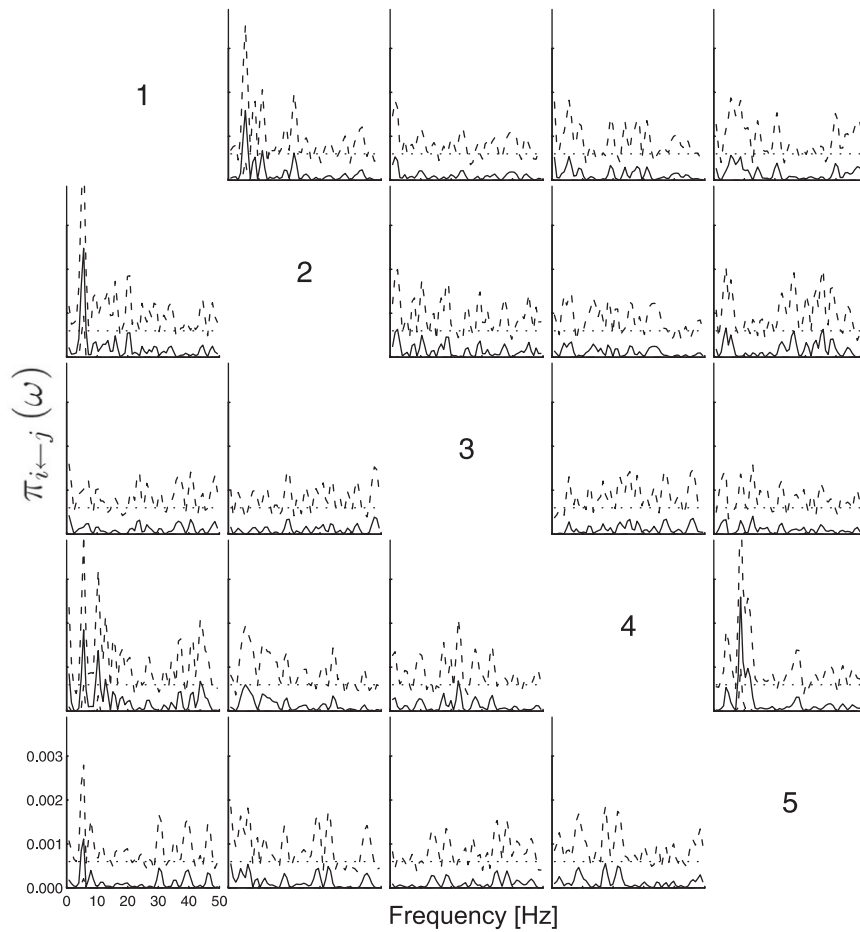


**Fig. 5.** Estimates of the rPDC for the considered neuron-EMG network. The rPDC values are arranged as in Fig. 4. The first four processes represent different neurons of the STN, while the fifth process belongs to the muscular activity. The coefficient  $\pi_{5 \leftarrow 1}$  indicates a direct directed influence from neuron 1 onto the muscle at approximately 5 Hz which was the trembling frequency of the muscle. Moreover the subthalamic nucleus is receiving proprioceptive input from the muscle as depicted in  $\pi_{4 \leftarrow 5}$ .

The representative results of a system consisting of four neurons and the activity of the trembling muscle is depicted in Fig. 5. The first four processes represent different neurons of the STN, while the fifth process displays the muscular activity. The tremor frequency in this example is 5 Hz. The results show, for instance, a strong influence from neuron 1 onto the muscular activity at the tremor frequency. Since there is also a highly significant influence from the muscular activity onto the neuronal activity of neuron 4 at the first higher harmonic of the tremor frequency, a feedback from the muscular activity to the STN is strongly suggested. Several neurons are also directly interacting with one another. These findings strongly support the assumption that the STN is involved in a tremor network to a large extent. It may moreover serve as a generator for tremor. Please note, however, that we do not claim a direct interaction between the neurons and the muscles. The information might well be mediated by unobserved brain structures like the sensori-motor-cortex. These structures were not recorded as there was no clinical need for such recordings.

## 7 Discussion

Nowadays data are gathered with a high temporal as well as spatial resolution. Moreover, modern recording devices are capable to deliver signals originating directly from neurons, which

can be treated as point processes. Thus, multivariate analysis techniques are desired being able to analyse point processes, time series and hybrids thereof. In this manuscript, we addressed possible analysis techniques to cope with these challenges. The presented modifications of the multivariate partial coherence and renormalised partial directed coherence allow for the analysis of networks consisting of point processes and time series. We demonstrated their abilities in a simulated network of neurons and applied them to physiological data. Novel insights into the generation of tremor in Parkinson's disease will emerge from the analysis of the data obtained during stereotactic neurosurgery.

The univariate, bivariate as well as multivariate techniques presented here are by no means restricted to the tremor application. Whenever point processes, time series or networks consisting of both are to be analysed, these methods will allow the rigorous assessment of the characteristics of the processes themselves and their interaction structure. False positive conclusions to the underlying dynamics are prevented using especially multivariate approaches.

## References

1. B. Schelter, M. Winterhalder, B. Hellwig, B. Guschlbauer, C.H. Lücking, J. Timmer, *J. Physiol.* **99**, 37 (2006)
2. R. Dahlhaus, *Metrika* **51**, 157 (2000)
3. D.R. Brillinger, *Time Series: Data Analysis and Theory* (Holden-Day, Inc., San Francisco, 1981)
4. P.J. Brockwell, R.A. Davis, *Time Series: Theory and Methods* (Springer, New York, 1991)
5. A.S. French, A.V. Holden, *Kybernetik* **8**, 165 (1971)
6. D.M. Halliday, J.R. Rosenberg, A.M. Amjad, P. Breeze, B.A. Conway, S.F. Farmer, *Prog. Biophys. Molec. Biol.* **64**, 237 (1995)
7. D.R. Brillinger, *The Spectral Analysis of Stationary Interval Functions*, edited by L.M. LeCam, J. Neyman, E. Scott, *Proceedings 6<sup>th</sup> Berkeley Symposium Mathematics Statistics Probability* (1972), p. 483
8. M.B. Priestley, *Spectral Analysis and Time Series* (Academic Press, London, 1989)
9. P. Bloomfield, *Fourier Analysis of Time Series: An Introduction* (John Wiley & Sons, New York, 1976)
10. L.A. Baccala, K. Sameshima, *Biol. Cybern.* **84**, 463 (2001)
11. K. Sameshima, L.A. Baccala, *J. Neurosci. Meth.* **94**, 93 (1999)
12. B. Schelter, M. Eichler, J. Timmer (submitted)
13. R.Q. Quiroga, Z. Nadasdy, *Neural Comput.* **16**, 1661 (2004)